

International Journal of Modern Physics: Conference Series
© World Scientific Publishing Company

Preparing single ultra-cold antihydrogen atoms for the free-fall in GBAR

LAURENT HILICO, JEAN-PHILIPPE KARR, ALBANE DOUILLET

*Département de Physique, Université d'Evry Val d'Essonne
Rue du père André Jarlan
Evry 91025, France*

Laboratoire Kastler Brossel UMR 8552, UPMC, CNRS, ENS, C 74, Université Pierre et Marie Curie

4 place Jussieu, Paris, 75252, France

Laurent.hilico@lkb.upmc.fr, jean-philippe.karr@lkb.upmc.fr, albane.douillet@lkb.upmc.fr

PAUL INDELICATO

Laboratoire Kastler Brossel UMR 8552, UPMC, CNRS, ENS, C 74, Université Pierre et Marie Curie

4 place Jussieu, Paris, 75252, France

paul.indelicato@lkb.upmc.fr

SEBASTIAN WOLF and FERDINAND SCHMIDT KALER

*QUANTUM, Institut für Physik, Universität Mainz, D-55128 Mainz, Germany
fsk@uni-mainz.de, wolfs@uni-mainz.de*

Received Day Month Year

Revised Day Month Year

We discuss an experimental approach allowing to prepare antihydrogen atoms for the GBAR experiment. We study the feasibility of all necessary experimental steps: The capture of incoming $\bar{\text{H}}^+$ ions at keV energies in a deep linear RF trap, sympathetic cooling by laser cooled Be^+ ions, transfer to a miniaturized trap and Raman sideband cooling of an ion pair to the motional ground state, and further reducing the momentum of the wavepacket by adiabatic opening of the trap. For each step, we point out the experimental challenges and discuss the efficiency and characteristic times, showing that capture and cooling are possible within a few seconds.

Keywords: sympathetic cooling, antihydrogen positive ion, antiprotonic atom, antimatter, Beryllium ion, Coulomb crystal, molecular dynamics simulations, gravitation

PACS numbers:37.10.Rs,36.10.-k,04.80.Cc,36.10.Gv

1. Introduction

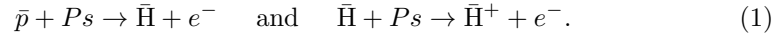
The GBAR project aims at measuring the earth gravity acceleration hereafter denoted \bar{g} felt by an antihydrogen atom $\bar{\text{H}}$, using a free-fall technique at first^{1,2,3} and possibly spectroscopy of $\bar{\text{H}}$ gravitational states in the future^{4,5}. Other collaborations AEGIS⁶, ATHENA-ALPHA⁷, ATRAP⁸ pursue the same goal using different

2 *L. Hilico & al.*

methods. The specificity of the GBAR project is to prepare a single antihydrogen atom at a temperature of the order of 10 μK , to obtain a sub-percent accuracy⁹ on \bar{g} . After a brief explanation of the scheme proposed for the GBAR experiment, we discuss in detail the trapping and sympathetic cooling of antihydrogen ions.

In the GBAR experimental scheme^{1,3}, neutral antihydrogen is prepared by photodetachment of the excess positron of a sympathetically cooled $\bar{\text{H}}^+$ trapped ion. The photodetachment is performed using a pulsed laser. The start time of the free-fall is the photodetachment pulse time. The stop time corresponds to the annihilation of the $\bar{\text{H}}$ on the detection plate. Obviously, reducing the velocity spread of $\bar{\text{H}}^+$ atoms is indispensable for determining \bar{g} with high precision.

The $\bar{\text{H}}^+$ ions are produced in two steps in a collision cell by sending keV antiprotons from the ELENA ring on a room temperature positronium cloud. The first step produces antihydrogen atoms and the second one the $\bar{\text{H}}^+$ ions following the reactions:



The reaction cross sections have been evaluated by P. Comini et al.¹⁰, predicting that bunches of a few $\bar{\text{H}}^+$ can be produced using state-of-the-art Ps sources. Since positronium is much lighter than \bar{p} , the $\bar{\text{H}}^+$ energy distribution is linked to that of the \bar{p} bunch produced by the ELENA ring¹¹ (whose expected characteristics are 100 keV mean energy and a 4π mm mrad emittance). The \bar{p} bunch is decelerated to an energy of a few keV using a drift tube. The kinetic energy spread of the \bar{p} bunch and hence of the $\bar{\text{H}}^+$ ion bunch is about 300 eV corresponding to a temperature of 2.3×10^6 K.

The relative resolution on \bar{g} that can be obtained measuring the free-fall time of a single particle is given by⁹

$$\frac{\Delta\bar{g}}{\bar{g}} = 2\sqrt{\left(\frac{\Delta\zeta}{2H}\right)^2 + \left(\frac{\Delta v}{\sqrt{2gH}}\right)^2} \quad (2)$$

where $\Delta\zeta$ and Δv are the position and velocity dispersions in the vertical direction. In the case of a quantum particle at the Heisenberg limit, $\Delta\zeta$ and Δv are linked by the uncertainty relation $m\Delta v\Delta\zeta = \hbar/2$ where m is the $\bar{\text{H}}$ inertial mass. An optimum resolution $(\Delta\bar{g}/\bar{g})_{opt} = 2^{1/4}\hbar^{1/2}m^{-1/2}\bar{g}^{-1/4}H^{-3/4}$ is obtained for $\Delta v_{opt} = 2^{-3/4}\hbar^{1/2}m^{-1/2}\bar{g}^{1/4}H^{-1/4}$ leading to $\Delta v_{opt} = 2.6$ mm/s and $(\Delta\bar{g}/\bar{g})_{opt} = 1.7 \times 10^{-4}$ assuming $\bar{g} = g$ and $H = 1$ m.

The recoil due to the absorption of the 1.64 μm detachment photon is $h/(m\lambda) = 23$ cm/s and may be set in the horizontal plane so that its influence on the free-fall vanishes. The recoil due to the excess energy can be made small using threshold detachment. The associated energy is 0.3 m/s under the realistic assumption that the photon energy is 1 μeV above detachment threshold. Thus photodetachment prevents reaching the optimal free-fall conditions even if the initial ion were perfectly motionless. Our goal vertical velocity dispersion is $\Delta v \approx 1$ m/s, Eq. 2 is then

dominated by the second term leading to $\Delta\bar{g}/\bar{g} = \sqrt{2}\Delta v/\sqrt{\bar{g}\bar{H}} = 0.4$ per detected atom. A 1% resolution can be obtained by averaging on 1600 events.

A transverse initial velocity of the order of 1 m/s is also required to avoid a too large detection area for the $\bar{\text{H}}^+$ annihilation plates. Those velocities correspond to energies of the order of 5.2 neV or 120 μK per degree of freedom. The $\bar{\text{H}}^+$ cooling challenge is to bridge a 10 to 11 orders of magnitude gap on the ion temperature, going from the classical world of particle beam physics to the ultimate frontiers of quantum world. Indeed, if one considers the ground state of a quantum harmonic oscillator of mass $m = 1$ a.u. and angular frequency ω , the velocity spread is given by $\Delta v = \sqrt{\hbar\omega/2m}$. $\Delta v = 1$ m/s leads to $\omega = 2\pi \times 5$ MHz. This is the typical secular motion frequencies that are achieved in ion traps, showing that the GBAR requirements can only be satisfied using ground state cooling techniques¹².

$\bar{\text{H}}^+$, antimatter equivalent of H^- , is extremely fragile against collisions with regular matter such that buffer gas cooling is not possible. Moreover, $\bar{\text{H}}^+$ is a single electronic level atom that cannot be directly laser cooled. Hence, we propose to use sympathetic cooling by the lightest laser cooled ion: $^9\text{Be}^+$.

2. Antihydrogen positive ion capture and Doppler cooling

Since only a few $\bar{\text{H}}^+$ ions are expected in each bunch, a nearly 100% capture efficiency is required. To that end, the GBAR project will first use capture and Doppler laser cooling step in a mm scale RF linear trap before transferring a single $\bar{\text{H}}^+$ ion into a miniaturized trap (called precision trap in the following) to perform ground state cooling of a $\text{Be}^+/\bar{\text{H}}^+$ ion pair. In Sect. 2, we discuss the capture and sympathetic cooling of a $\bar{\text{H}}^+$ ion in a big Be^+ crystal. In Sect. 3, we discuss the separation of the cold $\bar{\text{H}}^+$ ion and injection in the precision trap for ground state sideband sympathetic cooling before neutralization and $\bar{\text{H}}$ release.

2.1. $\bar{\text{H}}^+$ ion capture

The capture apparatus is depicted in Fig. 1. It is made of a RF quadrupole guide and a biased segmented linear trap described below. If the \bar{p} are not precooled below 300 eV, the kinetic energy spread of the $\bar{\text{H}}^+$ ion bunch is large, and requires a deep trap. The trapping depth of a linear trap is given by $U_{max} = qV_{RF}/8$ where q is the stability parameter and V_{RF} the applied voltage. The q parameter is inversely proportional to the ion mass and is typically chosen between 0.05 and 0.6 (larger values lead to important RF heating of the ions). In order to safely trap both Be^+ and $\bar{\text{H}}^+$, q must be chosen close to 0.45 for $\bar{\text{H}}^+$ and 0.05 for Be^+ . We assume a trapping depth of 20 eV for $\bar{\text{H}}^+$ that is obtained using $V_{RF} = 356$ V (712 V peak to peak). The stability parameter of a linear trap is given by $q = 2QV_{RF}/m\Omega^2r_0^2$ where m and Q are the ion mass and charge, r_0 is the inner trap radius, and Ω the RF frequency. With $r_0 = 3.5$ mm, we get $\Omega = 2\pi \times 17.7$ MHz, i.e., standard trap parameters. Efficient capture of $\bar{\text{H}}^+$ ions with a 300 eV kinetic energy spread

4 *L. Hilico & al.*

is much more involved, requiring 10 800 V peak to peak at 68.5 MHz. The use of RF traps with 2 drive frequencies¹³ was envisaged but it requires 2-3 order of magnitude different mass-to-charge ratios.

The incoming \bar{H}^+ ion bunch has 1 to 6 keV kinetic energy. The ion bunch is decelerated by biasing the linear trap by $U_b = 980$ to 5980 V. The trap input endcap voltage is lowered to U_b for a short time τ for the \bar{H}^+ ion bunch intake. Since the Be^+ ion motion is strongly damped by the cooling laser, and τ is much shorter than the axial trap secular period, the Be^+ ions don't have time to escape the trap. Figure 2-a shows a simulation of the capture efficiency (without Be^+) versus the time delay τ . 100% capture efficiency is predicted for a large range of τ for a small kinetic energy spread $\Delta E = 1$ eV. Figure 2-b shows the capture efficiency for optimal intake time τ versus the \bar{H}^+ bunch kinetic energy spread ΔE . The efficiency decreases with ΔE , but remains larger than 50% for $\Delta E < 25$ eV. This analysis shows that the initial kinetic energy spread of antiprotons from the ELENA source has to be reduced by at least one order of magnitude to allow for their efficient capture with reasonable trap parameters.

2.2. Sympathetic Doppler cooling time

Once captured, \bar{H}^+ ions have a very high temperature, limited by the trap depth. Next, they are sympathetically cooled by Coulomb interaction with a large laser cooled Be^+ ion cloud.

Because of possible photodetachment by the cooling laser light (see Sect. 2.3), it is very important to evaluate the cooling time. Sympathetic cooling dynamics results from the competition between the Coulomb repulsion and the trapping forces that take the ions together, and between laser cooling and RF heating. For this reason, it can only be evaluated using ion dynamics numerical simulation taking into account the exact time-dependent trapping forces responsible for micromotion and RF heating, and the exact Coulomb repulsion¹⁴. Short time steps (sub-ns range)

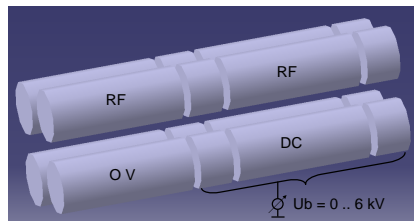


Fig. 1. Quadrupole guide and biased linear RF Paul trap used to decelerate and trap the \bar{H}^+ ion bunch. $L = 30$ mm.

must be used to well represent the fast dynamics due to the RF field and secure calculation convergence, since long simulation times are required to get sympathetic cooling evidence. The main numerical complication comes from the evaluation of the full Coulomb interaction for a large number of ions.

The numerical simulations are done using a home built FORTRAN code to solve the Newton's equation of motion for N_{lc} laser cooled Be^+ ions and N_{sc} sympathetically cooled ions, whose masses were taken equal to 1 ($\bar{\text{H}}^+$), 2 (H_2^+) and 3 (HD^+) in order to study the mass dependence of the cooling process. The equations are integrated using either a fixed-step fourth-order Runge-Kutta method or the leap-frog (Verlet-velocity)¹⁵ algorithm. The code takes into account the time-dependent RF trapping field and the axial harmonic trapping field of an ideal linear trap model given by the gradient of the potential

$$V(x, y, z, t) = (U_0 + V_{\text{RF}} \cos(\Omega t)) \frac{x^2 - y^2}{2r_0^2} + m_i \omega_{i,z}^2 (z^2 - (x^2 + y^2)/2), \quad (3)$$

where V_{RF} is the RF voltage, Ω the RF angular frequency, r_0 is the effective inner radius of the ion trap, $m_{(i)}$ is the mass of the considered ion and $\omega_{i,z}$ its axial oscillation frequency. For two different ionic species labeled i and j , we have $m_i \omega_{i,z}^2 = m_j \omega_{j,z}^2$. The Coulomb force undergone by ion i is given by

$$\mathbf{F}_{\rightarrow i} = \sum_{j \neq i} \frac{q_i q_j}{4\pi\epsilon_0} \frac{\mathbf{r}_i - \mathbf{r}_j}{r_{ij}^3}. \quad (4)$$

The laser action is taken into account in terms of absorption, spontaneous and stimulated emission processes for a two-level atom in a Gaussian laser beam of waist w_0 and wave vector \mathbf{k} . At each time step and for each laser-cooled ion, depending

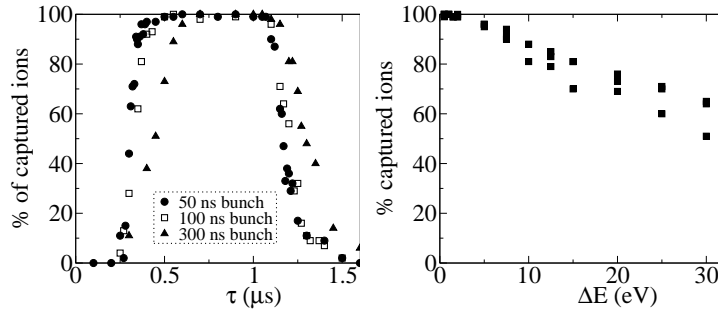


Fig. 2. (a): $\bar{\text{H}}^+$ capture efficiency versus trap opening time τ for different ion bunch durations, for $\Delta E = 1$ V. (b): $\bar{\text{H}}^+$ capture efficiency versus kinetic energy spread for $\tau = 0.9$ μs . Each point corresponds to a different simulation with 100 ions.

6 *L. Hilico & al.*

on its internal state and position in the laser beam, the absorption and emission probabilities are evaluated in a quantum jump approach. In case of absorption, stimulated or spontaneous emission, the ion velocity is changed by $\pm\hbar\mathbf{k}/m$ or by $\hbar\mathbf{k}\boldsymbol{\kappa}/m$ where $\boldsymbol{\kappa}$ is a random direction. At each time step, the ion positions are checked to be within a cylinder of radius r_0 and length L or are withdrawn from the simulation. The performance of the code is limited by the Coulomb interaction evaluation, so the computation time scales as the square of the ion number. The double precision Coulomb force subroutine evaluates 5×10^7 Coulomb terms per second on a 3 GHz CPU. Using multi-core CPU's, we observe a proportional speed-up.

A N_{lc} laser cooled Be^+ ion cloud is numerically prepared and relaxed to equilibrium, and N_{sc} $\bar{\text{H}}^+$ or H_2^+ ions are introduced along the trap axis, next to the Be^+ ion cloud (see Fig. 3) corresponding to a potential energy of a few meV. One can distinguish two cooling phases. At the beginning of the cooling process, the sympathetically cooled ion goes in and out the Be^+ ion cloud, and only periodically interacts with the coolant ions, progressively losing secular kinetic energy. During this first phase, the Be^+ ion cloud is not crystallized.

Once the sympathetically cooled ion gets embedded in the Be^+ cloud, a more efficient cooling phase then starts finally leading to a mixed species Coulomb crystal as shown in the left part of Fig. 3, which illustrates the second phase of the sympathetic cooling dynamics for a single H_2^+ or $\bar{\text{H}}^+$ ion by 2000 Be^+ laser-cooled ions. We plot the averaged macromotion kinetic energy in the x , y and z directions (see figure 3 caption). In the case of H_2^+ , we observe an exponential decay of the transverse kinetic energies down to the Doppler limit with a time constant of 1 ms, and a much faster decay of the axial kinetic energy, indicating the feasibility of fast sympathetic cooling for a 9/2 ion mass ratio. For $\bar{\text{H}}^+$, the situation is quite different. Whereas the axial motion is quickly damped to the Doppler limit, the competition between RF heating and sympathetic cooling in the transverse direction leads to a high transverse $\bar{\text{H}}^+$ kinetic energy corresponding to temperatures in the K range. Indeed, the motional coupling between two particles of different masses rapidly decreases with the mass ratio. It is thus important to work out more efficient sympathetic cooling schemes. One solution is to use an intermediate mass ion¹⁶ such as HD^+ with a mass of 3. The left part of Fig. 4 shows that starting with a Coulomb crystal made of 1800 Be^+ and 200 HD^+ ions, ms $\bar{\text{H}}^+$ cooling times are achievable.

2.3. Photodetachment constraints

The photodetachment threshold of $\bar{\text{H}}^+$ ($1.64 \mu\text{m}$) is well below the 313 nm Be^+ cooling photon energy, so the cooling laser beam may photodetach the excess positron. For a Be^+ cooling beam at saturation intensity ($I_{sat} = 2\pi^2\hbar c\Gamma/3\lambda^3 = 0.82 \text{ mW/mm}^2$ with $\Gamma = 2\pi \times 19.4 \text{ MHz}$), the photon flux is $\Phi = 7.9 \times 10^{16} \text{ photon/s/cm}^2$. The photodetachment cross section of H^- at 313 nm^{17,18} is $\sigma = 2 \times 10^{-17} \text{ cm}^2$, leading

to $\sigma\Phi = 1.6 \text{ s}^{-1}$. Under those conditions, the $\bar{\text{H}}^+$ lifetime is less than 1s. It can be made longer using a lower cooling intensity or by using a quasi continuous cooling beam with a reduced duty cycle. In a RF trap, the trapping effective potential is tighter for light ions than for heavy ones. Taking advantage of this fact, one might use a hollow laser beam in a Gauss-Laguerre mode¹⁹ L_0^1 to cool the Be^+ while the $\bar{\text{H}}^+$ ions which are strongly confined very close to the trap axis are exposed to a negligible amount of laser radiation at 313nm.

3. Ground state sympathetic cooling of a $\text{Be}^+/\bar{\text{H}}^+$ ion pair in the precision trap

As mentioned in the Introduction, the Doppler limit temperature is not low enough for the GBAR project, so the $\bar{\text{H}}^+$ ion will be injected in a precision trap to form a $\text{Be}^+/\bar{\text{H}}^+$ ion pair on which ground state Raman side band cooling can be performed¹².

The precision trap (see Fig 5)²³ consists of four gold coated, micro-fabricated alumina chips which are arranged in an x-shaped configuration and two endcaps

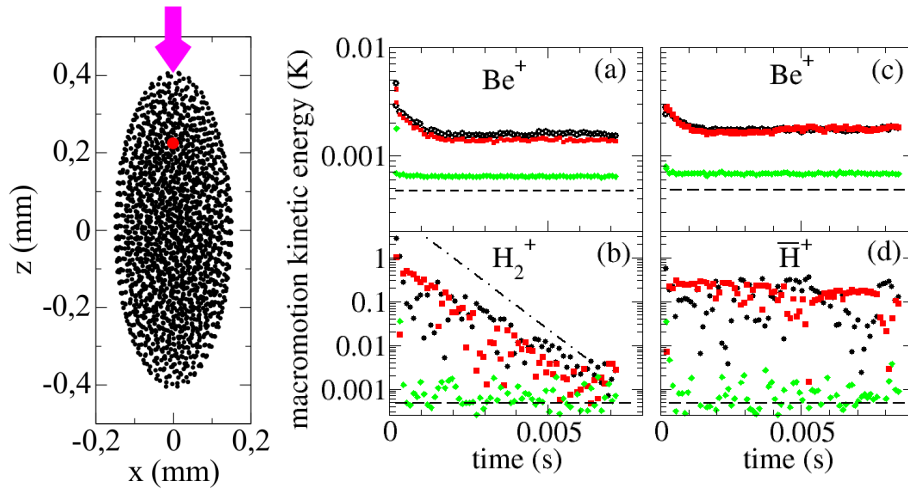


Fig. 3. **Left:** Snapshot of a 2000 Be^+ and 1 H_2^+ ion cloud. The sympathetically cooled H_2^+ ion is the red circle. The purple arrow shows the cooling laser direction. The cooling laser is aligned on the trap axis z with a waist $w_0 = 100 \mu\text{m}$ located at the trap center. The laser detuning is $-\Gamma/2$ and the laser intensity on the axis is I_{sat} . **Graphs:** Macromotion kinetic energy for each degree of freedom, averaged over 170 RF periods for 2000 laser cooled Be^+ ions (a,c) and for one H_2^+ (b) or $\bar{\text{H}}^+$ (d) sympathetically cooled ion. Black circles: x , red squares: y , green diamonds: z . The horizontal dashed line corresponds to the Doppler cooling limit temperature $k_B T_D = \hbar\Gamma/2$ leading to $k_B T_D/2 = 3.2 \times 10^{-27} \text{ J}$. The dash-dotted line in (b) corresponds to a 1 ms exponential decay behavior. For all the graphs, the trap parameters appearing in Eq. (3) are: $r_0 = 3.5 \text{ mm}$, $U_0 = 1 \text{ V}$, and $\Omega = 2\pi \times 17 \text{ MHz}$. The integration time step is $2 \times 10^{-10} \text{ s}$. (a) and (b): $V_{\text{RF}} = 356 \text{ V}$, $\omega_z = 500 \text{ kHz}$ for $m = 1$. (c) and (d): $V_{\text{RF}} = 200 \text{ V}$, $\omega_z = 300 \text{ kHz}$ for $m = 1$.

8 *L. Hilico & al.*

made from titanium. The endcaps are pierced with a hole with a diameter of $600 \mu\text{m}$ to enable ion injection into the trap. Two of the chips provide the RF-field and two the DC trapping potential respectively. The chips have 11 electrodes each to shape the axial potential what for the voltages can be controlled with a custom built digital-to-analog converter with a voltage resolution of $300 \mu\text{V}$ and a time resolution of 400 ns . The distance between the chips is $960 \mu\text{m}$. The trap is driven by an RF-voltage with a frequency $\Omega = 2\pi \times 56 \text{ MHz}$ and a peak-to-peak amplitude $V_{RF} = 176 \text{ V}$. This leads to a q parameter for Be^+ of 0.05 and for $\bar{\text{H}}^+$ of 0.45 . The center DC-electrode is held at -1.5 V to provide axial confinement. This voltage configuration leads to a axial and radial secular frequencies $\omega_z = 2\pi \times 1.9 \text{ MHz}$ and $\omega_{x,y} = 2\pi \times 8.7 \text{ MHz}$ for $\bar{\text{H}}^+$. The corresponding ground state kinetic energies are 0.09 and 0.41 mK .

After extraction from the capture trap, a cold $\bar{\text{H}}^+$ ion is injected into the precision trap through the end cap. The right part of Fig. 4 shows sympathetic Doppler cooling of a Be^+/X^+ ion pair where the precision trap is modeled as an ideal linear Paul trap. The cooling time strongly depends on the X^+ mass and can be larger than seconds in the case of $\bar{\text{H}}^+$. Again, the z -motion cooling is much faster due to the absence of RF heating.

In the precision trap, the cold Be^+ and $\bar{\text{H}}^+$ ions are coupled harmonic oscillators. The Doppler limit temperature (0.47 mK) corresponds to excitations of a few quanta that can be further laser cooled. The motional couplings of an ion pair confined in a RF Paul trap have been evaluated by Wübbena et al.²⁰. In the x , y or z directions, the individual ion trajectories can be expanded on *in-phase* and *out-of-*

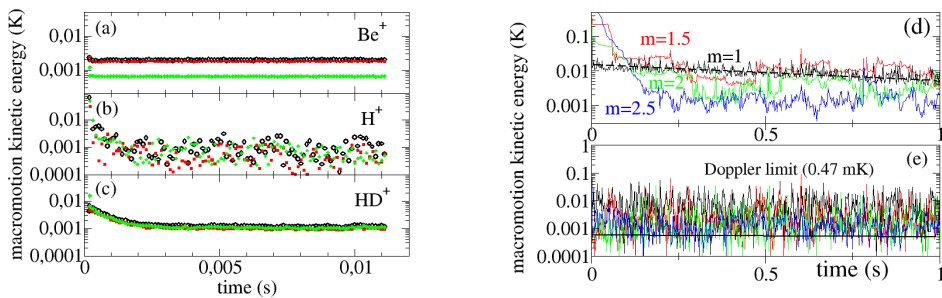


Fig. 4. **Left:** Sympathetic cooling dynamics of a $1800 \text{ Be}^+ / 200 \text{ HD}^+ / 1 \bar{\text{H}}^+$ mixed ion cloud. Numerical parameters as in Fig. 3(d). The $\bar{\text{H}}^+$ initial position is on the trap axis, 0.5 mm from the center, corresponding to a 4.6 meV potential energy. **Right:** Doppler cooling dynamics of a Be^+/X^+ ion pair in the precision trap. The mass of the sympathetically cooled ion corresponds either to real (black $m = 1$, green $m = 2$) or fictitious ion masses (blue $m = 2.5$, red $m = 1.5$). (d) 3D kinetic energy, (e) kinetic energy of the z motion.

phase eigenmodes as

$$u_1(t) = b_1 z_{in} \sin(\omega_{in} t + \phi_{in}) + b_2 z_{out} \sin(\omega_{out} t + \phi_{out}) \quad (5)$$

$$u_2(t) = \sqrt{\frac{m_1}{m_2}} b_2 z_{in} \sin(\omega_{in} t + \phi_{in}) - \sqrt{\frac{m_1}{m_2}} b_1 z_{out} \sin(\omega_{out} t + \phi_{out}), \quad (6)$$

where the amplitudes z_{in} and z_{out} and phases ϕ_{in} and ϕ_{out} depend on the initial conditions. The motional coupling coefficients b_1 and b_2 depend on the particle masses and trapping conditions and verify $b_1^2 + b_2^2 = 1$ (see Eq. (14) and (17) in²⁰). For the axial motion, we get $b_{1,z} = 0.982$ and $b_{2,z} = 0.187$. For the transverse motion, assuming $\omega_{x,y} = 1.1 \omega_z$, we get $b_{1,x,y} = 0.99971$ and $b_{2,x,y} = 0.017$, which can be compared to $1/\sqrt{2} \approx 0.707$ in the case of an ion pair with equal masses, or 1 for a single ion. Figure 5 shows the Be^+ electronic energy levels with the confined ion vibrational structure. Raman side band cooling consists in using an off-resonance stimulated Raman transition and a resonant spontaneous Raman transition to decrease the vibration number down to 0. A stimulated Raman transition is a coherent process. The time required to drive a π -pulse is inversely proportional to the dipole matrix element, i.e. to the coupling coefficient b_2 . For a $\text{Be}^+/\bar{\text{H}}^+$ ion pair, it is at most 60 times longer than for a single ion. In the latter case, Raman sideband cooling to the ground state for the three degree of freedom can be performed within a few tens of ms^{21,22}. For a $\text{Be}^+/\bar{\text{H}}^+$ ion pair, it may thus be achieved for the 6 degrees of freedom within 1 s.

Eigenmodes with frequencies in the 2-8 MHz range make it possible to efficiently laser cool the ion pair to its vibrational ground state. The corresponding velocity dispersion is still slightly too large for the GBAR experiment. We thus propose to adiabatically ramp down the trapping stiffness down to ≈ 30 kHz radial and longitudinal oscillation frequencies by slowly lowering the trapping voltage within about 500 ms. 30 kHz oscillation frequencies correspond to $\Delta v \approx 8$ cm/s velocity dispersions which amply satisfies the GBAR requirements.

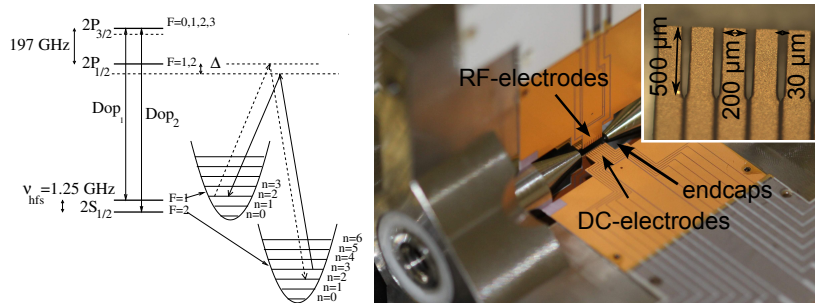


Fig. 5. **Left:** Energy levels of a $\text{Be}^+/\bar{\text{H}}^+$ ion pair including the ground and excited level of Be^+ and showing the harmonic ladder of one of the motional eigenmodes. The thin solid arrows show the Doppler cooling and repumping transitions. The thick solid arrows show the stimulated Raman transition, and the dashed arrows the spontaneous Raman transition. **Right:** Miniaturized trap of similar geometry to the precision trap to be used in the GBAR experiment.

4. Conclusion and perspectives

We have discussed the challenges and feasibility of antihydrogen positive ion $\bar{\text{H}}^+$ sympathetic cooling down to μK temperatures for the GBAR project. We here summarize the results.

- Capture efficiency of a 1 keV $\bar{\text{H}}^+$ ion bunch in a biased linear trap can be larger than 50% with a 25 eV kinetic energy dispersion and a trap depth of 20 eV. The efficient capture of an ion bunch with 300 eV dispersion requires out-of-reach trapping conditions, indicating that the antiprotons delivered by the ELENA ring have to be cooled beforehand to decrease the energy dispersion by at least a factor of 10.
- Sympathetic Doppler cooling by laser cooled Be^+ ions is shown to be efficient if the ions remain embedded in the Be^+ ion cloud. This means that one has to use large Be^+ ion clouds filling the capture trap. The numerical simulations show that the cooling efficiency is much better with a 9/2 rather than with a 9/1 mass ratio. In the latter case, the efficiency is dramatically improved using a third species of mass 3, i.e. HD^+ ions. A possible experimental scheme is then to prepare a laser cooled Be^+ ion cloud and to inject HD^+ ions from an external ion source (in order not to increase the pressure in the vacuum chamber) before the $\bar{\text{H}}^+$ bunch intake. Sympathetic Doppler cooling of energetic $\bar{\text{H}}^+$ is the most challenging step and is still an open problem, which has to be tackled both experimentally and using numerical simulation. To that end and in order to perform numerical simulations of the cooling dynamics with large number of ions (> 10000), the code will be implemented on massively parallel Graphic Processing Units (GPU). From the experimental point of view, this step will be first tested using matter ions H_2^+ and H^+ (protons).
- The transfer of a single $\bar{\text{H}}^+$ ion from the capture trap to the precision trap, which was not discussed here, will be done using standard ion beam optics for injection through the drilled end cap. The experimental protocol will be worked out first with matter ions with Ca^+/Be^+ and then Be^+/H_2^+ and $\text{Be}^+/\text{protons}$ before being implemented on GBAR. Here, the main issue is to avoid heating the ion during the transfer to secure a fast re-capture and sympathetic Doppler cooling of the ion pair.
- We have shown that once a $\text{Be}^+/\bar{\text{H}}^+$ ion pair is prepared at the Doppler limit temperature, Raman sideband sympathetic cooling down to the vibrational ground state of the trap is feasible with less than one second, preparing a $\bar{\text{H}}^+$ ion with a velocity dispersion of about 1 m/s.
- The velocity dispersion can be decreased to about 10 cm/s by adiabatically ramping down the trapping stiffness by a factor of 100, within less than 0.5 s. At that point, the velocity dispersion of the antihydrogen produced by threshold photodetachment of the excess positron is dominated by the recoil due to the e^+ ejection.

Acknowledgments

We thank Jofre Pedregosa for helpful discussions and Dominique Delande for introducing us to OPEN MP parallelization. We also thank the COST action MP1001-IOTA, NanoK-Infra Resima grant and ANR/DFG ANR-13-IS04-0002-01 BESCOOL grant.

5. References

References

1. J. Walz and T. Hänsch, *General Relativity and Gravitation* **36**, 561 (2004).
2. P. Perez and Y. Sacquin. *Classical and Quantum Gravity* **29**, 18 (2012).
3. SPSC-P-342, Proposal to measure the Gravitational Behaviour of Antihydrogen at Rest, GBAR. CERN (2011).
4. A. Yu. Voronin, V. V. Nesvizhevsky, and S. Reynaud, *Phys. Rev. A* **85**, 014902 (2012).
5. G. Dufour, A. Gérardin, R. Guérout, A. Lambrecht, V. V. Nesvizhevsky, S. Reynaud, and A. Yu. Voronin, *Phys. Rev. A* **87**, 012901 (2013).
6. A. Kellerbauer et al., *Nuclear Instruments and Methods in Physics Research Section B* **266**, 351 (2008).
7. The ALPHA Collaboration and A. E. Charman. *Nature Communications* **4**, 1785 (2013).
8. G Gabrielse. *Technical Report* CERN-SPSC-2010-006.SPSC-SR-057, CERN, Geneva, Jan 2010.
9. Gabriel Dufour, Pascal Debu, Astrid Lambrecht, Valery Nesvizhevsky, Serge Reynaud and Alexei Voronin, to be published in the European Physical Journal C (2014). doi: 10.1140/epjc/s10052-014-2731-8
10. P. Comini and P.-A. Hervieux, *New Journal of Physics* **15**, 095022 (2013).
11. SPSC-P-338, ELENA: An Upgrade to the Antiproton Decelerator. CERN.
12. D. Leibfried, R. Blatt, C. Monroe, D. Wineland, *Reviews of Modern Physics* **75**, 281 (2003).
13. D. Trypogeorgos, C. Foot, <http://arxiv.org/abs/1310.6294>.
14. K. Lämmerzahl, S. Schiller, *Physical Review A* **68**, 053406 (2003).
15. L. Verlet, *Physical Review* **159**, 98 (1957).
16. C. B. Zhang, D. Offenberg, B. Roth, M. A. Wilson, and S. Schiller, *Phys. Rev. A* **76**, 012719 (2007).
17. S. Chandrasekhar, D. D. Elbert, *Astrophysical Journal* **128**, 633 (1958).
18. S. J. Smith, D. S. Burch, *Physical Review Letters* **2**, 165 (1959).
19. C. T. Schmiegelow, F. Schmidt-Kaler, *European Journal of Physics D* **66**, 157 (2012).
20. J. B. Wübbena, S. Amairi, O. Mandel, P. O. Schmidt, *Phys. Rev. A* **85**, 043412 (2012).
21. T. Rosenband, P. O. Schmidt, D. B. Hume, W. M. Itano, T. M. Fortier, J. E. Stalnaker, K. Kim, S. A. Diddams, J. C. J. Koelemeij, J. C. Bergquist, and D. J. Wineland *Physical Review Letters* **98**, 220801 (2007).
22. C. W. Chou, D. B. Hume, J. C. J. Koelemeij, D. J. Wineland, and T. Rosenband *Physical Review Letters* **104**, 070802 (2010).
23. W. Schnitzler, N. M. Linke, R. Fickler, J. Meijer, F. Schmidt-Kaler and K. Singer, *Physical Review Letters* **102**, 070501 (2009).